What are the reference strains of *Acinetobacter baumannii* referring to?

Chantal Philippe[1 *], Adam Valcek[2, 3 *], Clémence Whiteway[2, 3], Etienne Robino[2, 3], Kristina Nesporova[3], Mona Bové[4], Tom Coenye[4], Tim De Pooter[5, 6], Wouter De Coster [7, 8], Mojca Strazisar[5, 6], Johanna Kenyon[9] and Charles Van der Henst[1, 2, 3 #]

* These authors contributed equally to the study.

[#] Corresponding author: charles.vanderhenst@vub.vib.be

Affiliations

[1] Research Unit in the Biology of Microorganisms (URBM), NARILIS, University of Namur (UNamur), Belgium.

[2] Microbial Resistance and Drug Discovery, VIB-VUB Center for Structural Biology, VIB, Flanders Institute for Biotechnology, Brussels, Belgium.

[3] Structural Biology Brussels, Vrije Universiteit Brussel (VUB), Brussels, Belgium.

[4] Laboratory of Pharmaceutical Microbiology, Ghent University, Ghent, Belgium.

[5] Neuromics Support Facility, VIB Center for Molecular Neurology, VIB, Antwerp, Belgium.

[6] Department of Biomedical Sciences, University of Antwerp, Antwerp, Belgium.

[7] Applied and Translational Neurogenomics Group, VIB Center for Molecular Neurology, VIB, Antwerp, Belgium

22 [8] Applied and Translational Neurogenomics Group, Department of Biomedical Sciences,
23 University of Antwerp, Antwerp, Belgium
24 [9] School of Biomedical Sciences, and Infection and Immunity Program, Institute of Health and
25 Biomedical Innovation (IHBI), Faculty of Health, Queensland University of Technology,
26 Brisbane, Australia.

27

28 # Abstract

29 We assembled the whole genome sequence (WGS) of a collection of 43 non-redundant modern
30 clinical isolates and four broadly used reference strains of *Acinetobacter baumannii*.
31 Comparison of these isolates and their WGS confirmed the high heterogeneity in capsule loci,
32 sequence types, the presence of virulence and antibiotic resistance genes. However, a
33 significant portion of clinical isolates strongly differ when compared to several reference strains
34 in the light of colony morphology, cellular density, capsule production, natural transformability
35 and *in vivo* virulence. These genetic and phenotypic differences between current circulating
36 strains of *A. baumannii* and established reference strains could hamper the study of *A.*
37 *baumannii* as an entity. The broadly used reference strains led to the current state of the art of
38 the *A. baumannii* field, however, we propose that established reference strains in the *A.*
39 *baumannii* field should be carefully used, because of the high genetic and phenotypic
40 heterogeneities. In this study, we generated a collection of high-quality nucleotide sequences
41 of 43 modern and non-redundant clinical isolates with the corresponding multi-level phenotypic
42 characterizations. Beside the contribution of novel fundamental observations generated in this
43 study, the phenotypic and genetic data, along with the bacterial strains themselves, will be
44 further accessible using the first open access online platform called "Acinetobase". Therefore,

45 a rational choice of modern strains will be possible to select the ones that suit the needs of
46 specific biological questions.
47

48 Introduction

49 Antibiotics overuse, along with fewer new therapeutics, represents a major challenge for human
50 health (Hernando-Amado et al., 2019; Poirel and Nordmann, 2006). Multidrug-resistant (MDR)
51 bacteria are increasingly isolated around the world, leaving physicians increasingly facing no
52 therapeutic option (Murray et al., 2022). As a direct consequence, patients are currently dying
53 from previously treatable diseases. In this context, WHO and CDC prioritize problematic
54 bacterial pathogens for which antibiotic resistance significantly impacts human health (Centers
55 for Disease Control, 2019; Tacconelli et al., 2018). *Acinetobacter baumannii* (Whiteway et al.,
56 2022), a member of the ESKAPE multidrug-resistant and most problematic nosocomial
57 pathogens (de Oliveira et al., 2020), was designated as a top-priority and critical agent for which
58 therapeutic alternatives are urgently required (Tacconelli et al., 2018).
59 *A. baumannii* is a Gram-negative opportunistic bacterial pathogen that thrives in hospital
60 settings, especially in intensive care units where weakened patients are treated (Whiteway et
61 al., 2022). Beside their intrinsic and acquired antibiotic resistance, *A. baumannii* resistance to
62 desiccation and disinfectants render any decontamination strategy a real challenge (Chiang et
63 al., 2018). One key aspect sustaining the rapid spread of antibiotic resistance amongst *A.*
64 *baumannii* isolates is their natural competence (Vesel and Blokesch, 2021). *A. baumannii*
65 bacteria undergo horizontal gene transfer during which exogenous DNA is taken up and
66 integrated within the bacterial genome (da Silva and Domingues, 2016). As a direct
67 consequence, rapidly evolving *A. baumannii* bacteria show a dynamic genome, with an

68 estimated core (conserved) genome of only 16.5%, while 25% of the genome is unique to each
69 strain, having no counterpart in any other *A. baumannii* genome (Imperi et al., 2011).
70 However, despite their clinical relevance, *A. baumannii* bacteria remain poorly understood.
71 Especially, their virulence and non-antibiotic associated resistance (disinfectants, desiccation
72 etc.) still needs to be better characterized (Harding et al., 2017). One possible explanation for
73 this gap of knowledge is the heterogeneity amongst *A. baumannii* isolates, rendering the
74 multiple approaches of typing of this bacterial species, with as a proof-of-concept the huge
75 diversity of the polysaccharide capsules and the outer core of the lipooligosaccharide (LOS) in
76 *A. baumannii*, as well as two multilocus sequence typing (MLST) schemes (Gaiarsa et al.,
77 2019). The LOS is present in *A. baumannii* instead of the common lipopolysaccharide (LPS).
78 Unlike LPS, the LOS is lacking the O-antigen and is composed of lipid A with variable amounts
79 of inner and outer core sugars (Kenyon et al., 2014). The outer sugars of LOS show diversity
80 across strains, dependent on glycosyltransferases and nucleotide-sugar biosynthesis enzymes
81 encoded in a highly variable outer core locus (OCL) (Geisinger et al., 2019).
82 The lipid composition of the outer membrane is involved in resistance to desiccation by
83 retaining water and nutrients within the bacterial cell (Boll et al., 2015; Sarshar et al., 2021).
84 Bacterial capsules consist of a polysaccharide layer deposited as the outermost surface exposed
85 leaflet on prokaryotic cells, impacting the virulence and antibiotics, as well as non-antibiotics-
86 based resistance (Dong et al., 2006; Niu et al., 2019). The locus encoding the genes involved in
87 the production and the assembly of the polysaccharide capsule (KL) is chromosomally encoded
88 and typically ranges from 20 to 35 kb in size. Its genetic organization comprises three modules
89 (Kenyon and Hall, 2013) encoding (i) the export machinery consisting of three proteins; Wza,
90 Wzb, and Wzc, (ii) glycosyltransferases and the capsule processing genes (and optionally genes
91 for the synthesis and modification of complex sugars) and (iii), genes involved in the synthesis
92 of simple sugar substrates. Another part of the capsular polysaccharide (CPS) used in typing

93 schemes is the OCL of LOS. The LOS of the outer membrane is a major virulence component
94 in Gram-negative bacteria. The OCL, similarly as KL, is encoded chromosomally and to date
95 14 variants (differing in the presence or absence of genes encoding multiple
96 glycosyltransferases and other enzymes) were described. OCL types can be divided in two
97 groups (A or B) based on the presence of *pda1* and *pda2* genes (Kenyon et al., 2014). The OCL
98 consists of genes involved in the synthesis, assembly and export of complex oligosaccharides
99 that are then linked to lipid A to form the LOS (Kenyon and Hall, 2013).
100 Witnessing the high diversity amongst *A. baumannii* isolates, our approach aims at
101 investigating to which extend the use of reference strains actually reflects the dynamic nature
102 and intrinsic heterogeneity of these bacteria in general, at the phenotypic and genotypic level.
103 In this study, we assessed the phenotypic and genetic diversity levels of 43 *A. baumannii*
104 modern clinical isolates, and we compared them to established type strains of *A. baumannii* in
105 the field: AB5075, ATCC17978, ATCC19606 and DSM30011 which are widely used in
106 various studies (Bravo et al., 2016; de Silva et al., 2017; Jacobs et al., 2014; Roussin et al.,
107 2019).
108

109 Materials and Methods

110 **Modern clinical isolates, reference strains and phylogeny inference**

111 A non-redundant collection of 43 modern (not older than 8 years) clinical isolates from the
112 National Reference Center for Antibiotic-Resistant Gram-Negative Bacilli (CHU UCL-Namur)
113 and four established reference strains: ATCC17978-VUB, ATCC19606-VUB, DSM30011-
114 VUB and AB5075-VUB were studied. The reference strains AB5075, ATCC17978 and
115 ATCC19606 are non-MDR (except AB5075) strains of clinical (osteomyelitis, meningitis and
116 urine, respectively) origin (Gallagher et al., 2015; Harding et al., 2017) while DSM30011 is a
117 non-MDR environmental strain obtained from plant microbiota (Repizo et al., 2017). The

118 reference strains were designated with the extension "-VUB" in order to distinguish the strains
119 and their sequences examined within our study. The selected isolates were described in our
120 previous study (Valcek et al., 2021). In order to increase the heterogeneity of the collection,
121 three carbapenem-susceptible isolates (AB21-VUB, AB169-VUB and AB179-VUB) were
122 added and analyzed as well. We sequenced the whole genome of these isolates using shorts
123 reads (Illumina) combined with long reads [Oxford Nanopore Technologies (ONT)] sequencing
124 techniques to generate *de novo* assembled genomes for each of them.
125
126 **Short- and long-read sequencing**
127 Genomic DNA extraction and the sequencing library preparation for short-read 2x250 bp
128 paired-end MiSeq (Illumina) sequencing was performed as described before (Valcek et al.,
129 2021). The DNA for long-read MinION (ONT) sequencing was extracted using Genomic-tip
130 100/G (Qiagen, Hilden, Germany). The long-read sequencing libraries were prepared using 1D
131 Ligation Barcoding Kit (SQK-LSK109 and EXP-NBD104 ONT, Oxford, UK). Samples were
132 QCed using Qubit (dsDNA BR chemistry, Thermo Fisher Scientific), and Fragment Analyzer,
133 Agilent Technologies (using DNF-464 kit). Average size of the fragments was 45-70 kb.
134 Samples were equimolarly pooled and run per 12 in one run which was always 2x reloaded.
135 MinION flowcells had min. 1200 sequencable pores at the start and initial loading was
136 approximately 35 fmol followed by 2 reloads each after 24h into sequencing. The sequencing
137 was performed on MinION Mk1b (ONT) using R9.4.1 (FLO-MIN106) flowcells.
138
139 **Sequence data analysis**
140 The long-reads sequences were demultiplexed and basecalled using Guppy v3.2.2 and
141 subsequently were adaptor, quality (Q≤13) and length (5000 bp) trimmed using Porechop
142 v0.2.2 (https://github.com/rrwick/Porechop) and NanoFilt v2.8.0 (de Coster et al., 2018.),

143 respectively. The short reads (BioProject PRJNA734485) were used to polish the long reads
144 employing Ratatosk v0.7.0 (Holley et al., 2021). The corrected reads were then assembled using
145 Flye v2.9 (Kolmogorov et al., 2019) resulting in circular chromosomal contigs of all isolates.
146 The circularity was verified by mapping short reads to corresponding assemblies in order to
147 observer overlapping sequences. The circular chromosomal contigs were polished using long
148 reads via racon v1.4.20 (https://github.com/isovic/racon) and Medaka v1.2.2
149 (https://github.com/nanoporetech/medaka) and subsequently by quality (Q≤20) and adaptor
150 trimmed (using Trimmomatic (Bolger et al., 2014)) short reads in three rounds of Pilon (Walker
151 et al., 2014) polishing.
152
153 **Antimicrobial resistance genotype and phenotype**
154 The antimicrobial susceptibility testing and characterization of its genetic background was
155 performed and described in our previous study (Valcek et al., 2021).
156
157 **Natural competence of the isolates**
158 The natural competence of the clinical isolates and reference strains of *A. baumannii* was
159 assessed by starting an overnight bacterial culture from -80°C stock in 5mL of LB (37°C at 160
160 rpm). The culture was diluted 1:100 in 2mL microtube (10µL of the bacterial culture + 990µL
161 tryptone solution of 5g/L). Then 3µL of the diluted culture was mixed with 3µL of plasmid
162 DNA (100ng/µL) in 1mL microtube. Subsequently, 3µL of the mix of culture and plasmid DNA
163 was transferred to a 2mL microtube containing 1mL tryptone 5g/L agar 2%. A 3µL of diluted
164 bacterial culture without plasmid DNA was used as a negative control.
165 After 6h incubation at 37°C, 100µL of tryptone solution at 5g/L was added to the microtube
166 with the culture and plasmid DNA and vortexed gently. A 50µL of the suspension was plated
167 on LB agar plates containing apramycin (50µg/mL) to select transformants. The negative

168 control was plated apramycin LB agar plates too. Colonies were counted after overnight
169 incubation at 37°C.
170
171 **Hemolytic and protease activities**
172 To assess the potential hemolytic activities of the different *A. baumannii* isolates, we spotted 5
173 µl of an O/N (overnight) culture of bacteria previously grown in LB medium for 16 hours at
174 37°C under constant agitation (175 rpm) on 4 different Blood Agar Plates: (i) Columbia Agar
175 with 5% Horse Blood, (ii) Columbia Agar with 5% Sheep Blood, (iii) Trypticase^{TM} Soy Agar
176 II with 5% Horse Blood and (iv) Trypticase^{TM} Soy Agar II with 5% Sheep blood, all purchased
177 from BD (Becton, Dickinson and Company, Franklin Lakes, NJ). To test for secreted protease
178 activity, we used the same approaches as described above and spotted the 5 µl of bacteria on
179 LB agar plates containing 2% of Skim Milk Powder for microbiology (Sigma-Aldrich/Merck
180 KGaA, Darmstadt, Germany). Plates were incubated at 25°C and monitored for hemolytic and
181 protease activities after 1, 2 and 6 days of incubation.
182
183 **Phylogenetic analysis**
184 The maximum-likelihood tree depicting the relatedness of the isolates was constructed from
185 assembled complete genomes using precited open reading frames obtained by Prokka
186 (Seemann, 2014) as an input for the core-genome alignment created using Roary (Page et al.,
187 2015). RAxML (Stamatakis, 2006) was used for calculation of the phylogenetic tree using
188 general time reversible with optimization of substitution rates under GAMMA model of rate
189 heterogeneity method supported by 500 bootstraps. The phylogenetic tree was visualized in
190 iTOL (Letunic and Bork, 2019).
191
192 **Genotypic characterization**

193 The resistance and virulence genes were detected using ABRicate
194 (https://github.com/tseemann/abricate) employing ResFinder 4.1 (Bortolaia et al., 2020),
195 VFDB 2022 (Liu et al., 2022) and MEGARes 2.0 (Doster et al., 2020) databases, respectively
196 with 90% threshold for both gene identity and coverage. The typing of capsule-encoding loci
197 (KL) and lipooligosaccharide outer core (OCL) were determined using Kaptive (Wick et al.,
198 2018; Wyres et al., 2020) after manual curation of the corresponding loci by mapping the short
199 reads on anticipated reference sequence of the KL using Geneious R9 (Biomatters, NZ).
200

201 **Macrocolony morphology**

202 5 µl of overnight bacterial suspension (~ $1x10^8$ cells) was plated on Columbia Agar with 5%
203 Sheep Blood purchased from BD (Becton, Dickinson and Company, Franklin Lakes, NJ). The
204 plates were incubated non-inverted for 24h at 25°C and subsequently photographed by a
205 Canon® camera.
206

207 **Capsule production**

208 1 ml of overnight culture in a 1.5 ml microtube was centrifuged for 2 min at 7000 rcf. The
209 supernatant was removed, and the pellet was resuspended in 1 ml of PBS. Subsequently, 875
210 µl of PBS resuspended bacteria were mixed with 125 µl of LUDOX® LS colloidal silica (30
211 wt. % suspension in H_2O, Merk) (Ardissone et al., 2014; Kon et al., 2020). This mix was then
212 centrifuged for 30 min at 12.000 rcf and immediately photographically recorded.
213

214 **Transmission electron microscopy (TEM)**

215 Transmission electron microscopy (TEM) was used for direct capsule visualization by labeling
216 the capsule of 11 *A. baumannii* isolates, 9 modern clinical isolates and 3 reference strains, which
217 ranges from high to low densities. The fixation and staining of the bacteria were performed as

218 described before (Chin et al., 2018). The cupule with the fixed pellet of bacteria (polymerized
219 for 5 hours) was embedded in resin and polymerized (12h at 37°C, 48h at 45°C and 3 days at
220 60°C). The ~60 nm slides of the resin were marked with acetate uranyl and placed on the
221 electron microscopy grid.
222
223 **Virulence in *Galleria mellonella* model of infection**
224 TruLarv research grade larvae of *G. mellonella* (BioSystems Technology) were stored at 15°C
225 no longer than 5 days after arrival and were incubated for 30 min at 4°C prior to injection.
226 Bacteria from an overnight culture were washed with physiological saline (PS) (0.9% NaCl)
227 and diluted to approx. $1x10^7$ CFU/ml. The larvae were injected with 10 µl of PS containing
228 $1x10^5$ CFU/ml of *A. baumannii* in the last left proleg using a 0.3 ml insulin syringe (BD
229 MicroFine). Each of the nine selected strains of *A. baumannii* were injected into 10 larvae and
230 10 larvae were injected with PS as a negative control. The experiments were carried in
231 duplicates and the survival (assessed by keratinization and mobility) rate was evaluated each
232 day in a period of 5 days.
233

234 Results

235 **Genotypical characterization of the isolates**
236 We have previously described the sequence types (ST) and the antibiotic resistance profiles of
237 40 modern carbapenem-resistant clinical isolates of *A. baumannii* bacteria (Valcek et al., 2021).
238 We completed our strain collection by generating the whole genome sequence (WGS) of three
239 carbapenem-sensitive modern isolates (AB21-VUB, AB169-VUB and AB179-VUB) and four
240 broadly used reference strains in the *A. baumannii* field (AB5075-VUB, ATCC19606-VUB,
241 ATCC17978-VUB and DSM30011-VUB), their phylogenetic tree and antimicrobial resistance
242 genes (Supplementary Figure 1).

243 We further investigate the genetic background of our extended strain collection and generate
244 polished *de novo* assembled genomes by combining Illumina and Oxford Nanopore
245 Technologies sequencing data. Comparison of the whole genome sequences (WGS) of the 43
246 modern clinical isolates and four reference strains of *A. baumannii*, identified a core genome
247 containing 2009 genes (Figure 1), representing 14.76% of coding sequences (CDS) from the
248 pan-genome of 13611 CDS. The more *A. baumannii* genomes are analyzed, the more unique
249 genes are identified (Figure 2B) while the number of conserved genes decreased. These findings
250 confirm the great variability of *A. baumannii* bacteria, pointing towards a still open pan-genome
251 of *A. baumannii* bacteria that are often changing. Therefore, we still make the current prediction
252 that, every time a new isolate of *A. baumannii* is sequenced, most likely (a) novel gene(s) would
253 be identified.
254 We further analyzed the 47 genomes of our strain collection in regard to their respective
255 sequence type (ST), capsule locus type (KL) and lipooligosaccharide locus (OCL) types.
256 Twelve ST groups were identified, with ST2 as the most prevalent (25/43) followed by ST636
257 (6/43), ST1 (4/43), ST85 (2/43), ST78 (2/43) and ST604, ST215, ST158 and ST10 (one isolate
258 each) (Figure 2). The four reference strains belong to ST1 (AB5075-VUB), ST52
259 (ATCC19606-VUB), ST437 (ATCC17978-VUB) and ST738 (DSM30011-VUB). We found
260 that the most frequent capsule type was KL40 (10/43) followed by KL9 (6/43), KL3 (5/43),
261 KL2 (4/43), KL13 and KL4 (3/43), KL22 and KL6 (2/42) and KL125, KL124, KL81 KL58,
262 KL18, KL12, KL10 and KL7 (one isolate each) (Figure 2). We confirmed that the reference
263 strains ATCC19606-VUB and ATCC17978-VUB, both belonged to KL3, while DSM30011-
264 VUB to KL47 and AB5075-VUB to KL25 (Arbatsky et al., 2015; Senchenkova et al., 2015;
265 Wang-Lin et al., 2017). In this regard, the reference strains ATCC19606-VUB and
266 ATCC17978-VUB, both KL3, were more representative than DSM30011-VUB (KL47) and
267 AB5075-VUB (KL25) which were sole to be of said KL. The typing of the locus encoding the

268 OCL of the LOS revealed high occurrence of OCL1 (31/43) followed by OCL2 (7/43), OCL6
269 and OCL3 (2/43) and OCL5 (1/43). We confirmed that the reference strains belonged to OCL2
270 (AB5075-VUB and ATCC17978-VUB), OCL3 (ATCC19606-VUB) and OCL6 (DSM30011-
271 VUB).
272 The phylogenetic along with the genetic analyses of KL and OCL showed that, except for
273 AB5075-VUB, the reference strains ATCC17978-VUB, ATCC19606-VUB and DSM30011-
274 VUB only clustered with the clinical isolates of rare ST and KL. Despite AB5075-VUB was
275 sole of the KL25 it clustered closer to the modern clinical isolates of *A. baumannii*. In addition,
276 a variety of genes from operons encoding RND efflux pumps involved in virulence were not
277 present in said three oldest reference strains (ATCC19606-VUB, ATCC17978-VUB and
278 DSM30011-VUB), and a key gene involved in biofilm formation (*bap*) was undetected in all
279 reference strains (Figure 2). Employing MEGARes 2.0 database, only reference strain AB5075-
280 VUB encoded all three RND efflux pumps *adeIJK, adeABC,* and *adeFGH*, while DSM30011-
281 VUB, ATCC17978 and ATCC19606-VUB had an incomplete *adeABC* (lacking *adeC*, all three
282 strains) and/or *adeFGH* (lacking *adeF*, DSM30011-VUB, ATCC19606-VUB) operon. Besides
283 these three reference strains, only six modern clinical MDR strains of *A. baumannii* contained
284 one or more incomplete operons encoding RND efflux pumps.
285
286 **Figure 1 and 2.** Bottom of the file (horizontally oriented)
287
288
289 **Natural competence of *A. baumannii* clinical isolates and strains**
290 We next assessed the natural competence ability of all the *A. baumannii* strains. The reference
291 strain AB5075-VUB was used as a positive control due to its high competence in the tested
292 conditions (Le et al., 2021). We have categorized the strains in regard to its level of competence
293 (Table 1). These results are showing not only variability in the natural competence of the

294 clinical isolates and reference strains of *A. baumannii*, but also a different level of the natural
295 competence.
296
297 **Table 1:** A table summarizing number of colonies of *A. baumannii* clinical isolates and reference strains detected
298 after the transformation with plasmid containing apramycin cassette. High: >50 colonies; Medium: 30 – 50
299 colonies; Low: <5 colonies; Not detected – 0 colonies; in the tested conditions. ND – Not Detected.

Strain	Level of competence	Strain	Level of competence
DSM30011-VUB	Medium	AB181-VUB	ND
ATCC17978-VUB	ND	AB183-VUB	ND
ATCC19606-VUB	ND	AB186-VUB	High
AB3-VUB	ND	AB187-VUB	ND
AB9-VUB	ND	AB188-VUB	Low
AB14-VUB	ND	AB189-VUB	High
AB16-VUB	ND	AB193-VUB	ND
AB20-VUB	High	AB194-VUB	ND
AB21-VUB	ND	AB212-VUB	ND
AB32-VUB	Low	AB213-VUB	ND
AB36-VUB	ND	AB214-VUB	ND
AB39-VUB	ND	AB216-VUB	ND
AB40-VUB	ND	AB217-VUB	ND
AB167-VUB	ND	AB219-VUB	ND
AB169-VUB	High	AB220-VUB	ND
AB171-VUB	ND	AB222-VUB	High
AB172-VUB	ND	AB224-VUB	ND
AB173-VUB	ND	AB226-VUB	ND
AB175-VUB	ND	AB227-VUB	High
AB176-VUB	High	AB229-VUB	High
AB177-VUB	ND	AB231-VUB	ND
AB179-VUB	ND	AB232-VUB	High
AB180-VUB	ND	AB233-VUB	ND

300
301
302 **Colony morphology of *A. baumannii* and the need for classification to define new**
303 **phenotypic categories**

304 We have now confirmed the high heterogeneity at the genetic level amongst our strain
305 collection of MDR modern clinical isolates (Figure 1). To test whether this observation
306 correlates with different levels of phenotypic heterogeneity, we spotted each strain on different
307 blood and milk derived media and observed the potential hemolytic or secreted protease
308 activities (Van der Henst et al., 2018) as well as the ultrastructure of macrocolonies (Figure 3).
309 The clinical isolates and the reference strains did not show detectable hemolytic or protease
310 activities in the tested conditions, which is a common trait amongst *A. baumannii* bacteria
311 (Bouvet and Grimont, 1986) (Figure 1). The reference strains AB5075-VUB, DSM30011-
312 VUB, ATCC17978-VUB and ATCC19606-VUB do represent this common phenotypic trait,
313 despite the high genetic diversity observed, confirming that the tested modern clinical isolates
314 did not acquire increased hemolytic nor secreted protease activities. However, the analysis of
315 the macrocolonies morphology highlights an important diversity level of the modern clinical
316 isolates compared to the reference strains. As shown in Figure 3 and Table 2, we observed at
317 least five different categories of ultrastructure of macrocolony for the modern clinical isolates
318 and only two categories for the tested reference strains, with the more modern isolate AB5075-
319 VUB being different compared to the three other reference strains DSM30011-VUB,
320 ATCC17978-VUB and ATCC19606-VUB. We could identify six constitutive mucoid strains
321 in the macrocolony type (MT) "A" group of *A. baumannii* isolates (Figure 3B). The colonies
322 of the isolates with constitutive mucoid phenotype had circular shape and smooth margin. The
323 least frequent morphology of a colony and second most mucoid was circular with raised top of
324 darker white color with only three isolates, representing the MTB group (Figure 3B). The most
325 abundant (n=17) type of colony (MTC) was irregular with translucent bottom and opaque top
326 with irregular margin. This group also includes the most modern reference strain AB5075-VUB
327 (Figure 3A). The isolates of the MTD group (n=14) produced circular colonies with undulate
328 margin and volcano shaped center. Most of the reference strains belongs to the MTE group of

329 seven least mucoid isolates (Figure 3B) with circular shape, translucent center and opaque outer
330 ring. Hence, the shapes of the colonies allowed to divide the isolates into five macrocolony type
331 groups with one representative isolate depicted in Figure 3 (Table 2).

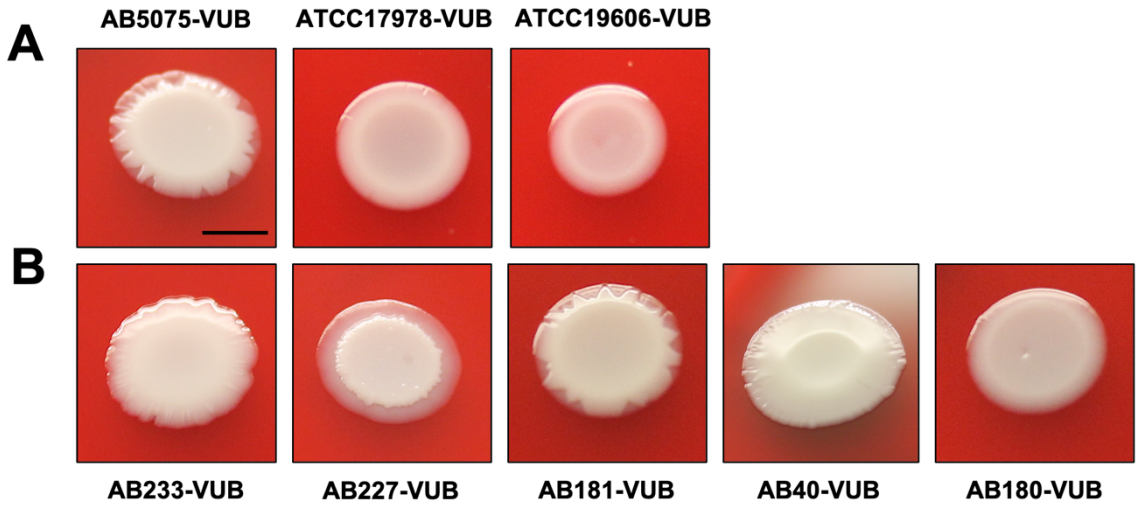

332

333 **Figure 3:** Diversity of the macrocolony types of the reference strains (A) compared to modern clinical isolates (B)
334 grown on columbia agar plates with 5% sheep blood. Scale bar: 1 cm.

335
336 **Table 2:** A table dividing the reference strains and the clinical isolates to five categories (MTA-MTE) based on
337 the colony morphology from the most mucoid phenotype (A) to the least mucoid phenotype (E). Each category is
338 represented by one isolate, which is depicted in Figure 3B.

Macrocolony Type (MT)	AB233-VUB **(MTA)**	AB227-VUB **(MTB)**	AB181-VUB **(MTC)**	AB40-VUB **(MTD)**	AB180-VUB **(MTE)**
	AB3-VUB	AB16-VUB	AB14-VUB	AB9-VUB	AB32-VUB
	AB39-VUB	AB20-VUB	AB21-VUB	AB36-VUB	AB212-VUB
	AB173-VUB		AB169-VUB	AB167-VUB	AB213-VUB
	AB177-VUB		AB171-VUB	AB175-VUB	ATCC17978-VUB
			AB172-VUB	AB176-VUB	ATCC19606-VUB
			AB186-VUB	AB179-VUB	DMS30011-VUB
			AB188-VUB	AB183-VUB	
			AB193-VUB	AB187-VUB	
			AB194-VUB	AB189-VUB	
			AB217-VUB	AB214-VUB	
			AB219-VUB	AB216-VUB	
			AB220-VUB	AB222-VUB	
			AB224-VUB	AB226-VUB	
			AB229-VUB		
			AB231-VUB		
			AB232-VUB		
			AB5075-VUB		

339

340

341 **Capsule production of *A. baumannii***

342 As the mucoid phenotype can reflect the presence of an abundant polysaccharide capsule
343 surrounding bacteria, we established a density gradient assay to assess encapsulation level of
344 all *A. baumannii* isolates in a medium to high throughput level (Figure 4) (Whiteway et al.,
345 2021). In this phenotypic assay, low density bacteria have a high capsulation level, while denser
346 bacteria have lower capsulation levels (Figure 4A). A high heterogeneity degree concerning the
347 density of *A. baumannii* bacteria, crossing the full range from low to high density levels is
348 observed (Figure 4D). Interestingly, four clinical isolates were divided into two fractions,
349 suggesting diversity in production of CPS even within the same isolate, possibly pointing
350 towards a high frequency of phase variation leading to phenotypic heterogeneity previously
351 described (Tipton et al., 2015). In majority, the reference strains show high densities except for
352 AB5075-VUB characterized by a medium density level. Despite having low capsulation levels,
353 the ATCC19606-VUB isolate constantly shows a lower density compared to the strain
354 ATCC17978-VUB. On the other hand, none of the high-density isolates belonged to KL40,
355 unlike majority of low-density producers, pointing towards causality. While in high density
356 isolates no other pattern than frequent occurrence of ST2 (10/15) was observed, the isolates of
357 low density were often of KL40 (7/9) of ST2 (5/9) or ST636 (4/9). In conclusion, we could not
358 attribute a specific cell density with the capsule type. The colony morphology (MTE) and the
359 density gradient of four modern clinical isolates of our collection (AB32-VUB, AB180-VUB,
360 AB212-VUB and AB213-VUB) resembles those of the low capsulated reference strains
361 ATCC17978-VUB, ATCC19606-VUB and DSM30011-VUB, hence was to a certain extent
362 represented by two reference strains. In this regard, the reference strain AB5075-VUB
363 represented 17 clinical isolates of MTC, yet the density gradients of this group were too
364 heterogenous to be represented by a sole reference strain AB5075-VUB. However, the majority

365 (n=22/43) of the modern clinical isolates was not represented by the reference strains of *A.*

366 *baumannii* considering the capsule production (density gradient) and macrocolony types.

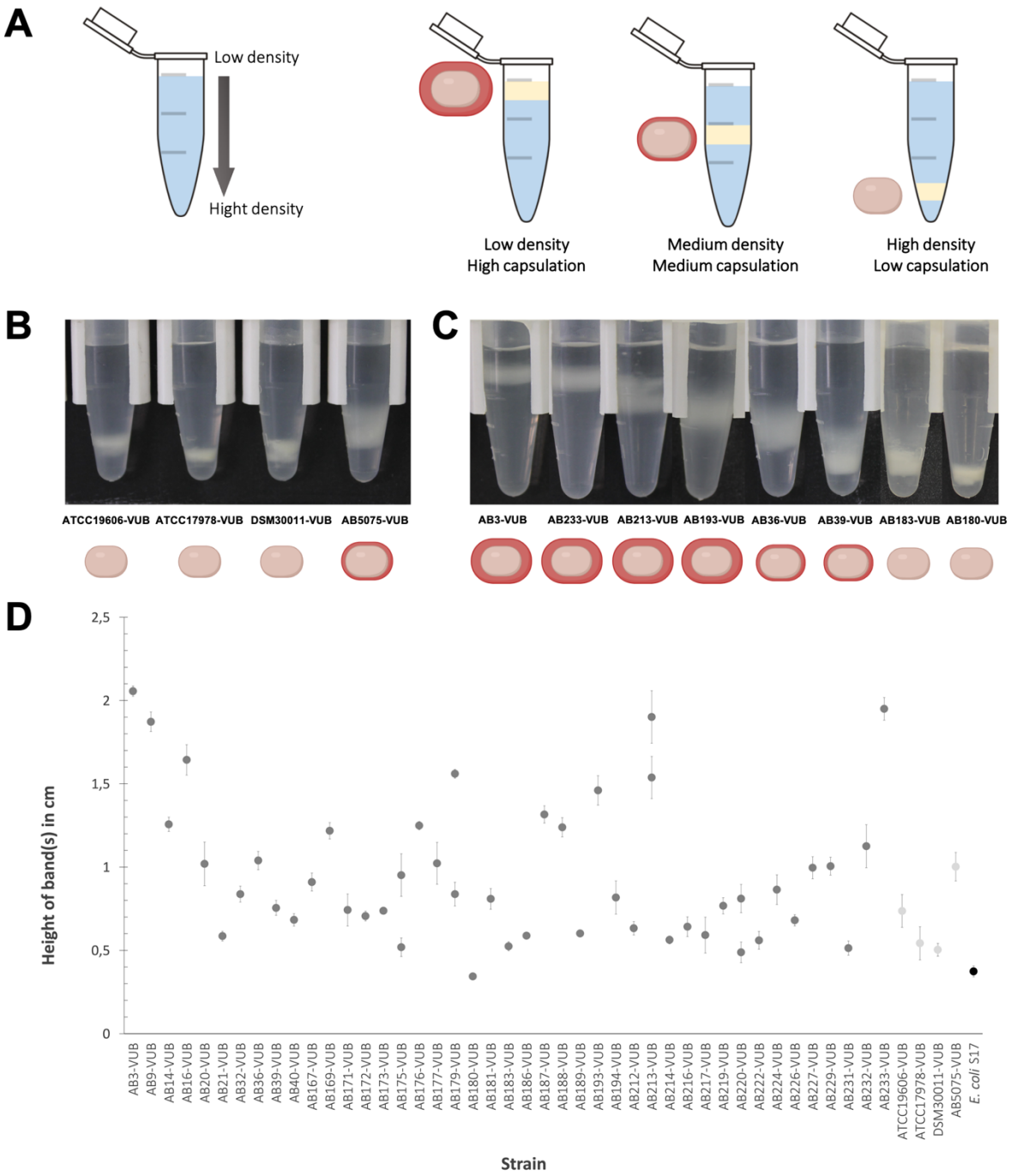

367

368 **Figure 4:** (A) Depiction of the density gradient measuring principle. (B) Capsulation level of the reference strains

369 and (C) comparison of various levels of capsulation of the modern clinical strains of *A. baumannii*. (D)

370 Quantification of the density of bacterial cells measured in a gradient colloidal silica; standard deviation was

371 calculated from biological triplicates.

372

373 To directly observe capsule deposition and thickness at high resolution and at the single cell
374 level, we combined capsule labeling with transmission electron microscopy (TEM) approach
375 (Figure 5). As expected, high density bacteria are surrounded by a denser and thicker capsule
376 compared to low density bacteria (Figure 5B). Concerning the reference strains, we confirm
377 AB5075-VUB to be the more capsulated reference strain tested in this study. We could not
378 detect any capsule deposition on the ATCC17978-VUB strain and the ATCC19606-VUB
379 shows weak and heterogeneously deposited layer in the tested conditions. This is in line with
380 the reference strain ATCC19606-VUB being less dense compared to the reference strain
381 ATCC17978-VUB in our density gradient assay (Figure 4D). Two less capsulated modern
382 strains, the AB180-VUB and AB183-VUB also show high densities (in density gradient assay)
383 with less abundant capsule deposition. The least dense isolates AB3-VUB, AB193-VUB and
384 AB213-VUB show a high abundance of capsule formation. Accordingly, the strains AB36-
385 VUB that shows an intermediate density level have an intermediate capsule deposition level
386 while the AB39-VUB strain reaches a higher density with less capsule deposition. Taken
387 together, these data show that bacterial density correlates with capsule abundance of *A.*
388 *baumannii* bacteria and that the reference strains does not show all the heterogeneity observed
389 in the modern clinical isolates tested regarding capsule production level.

390

391

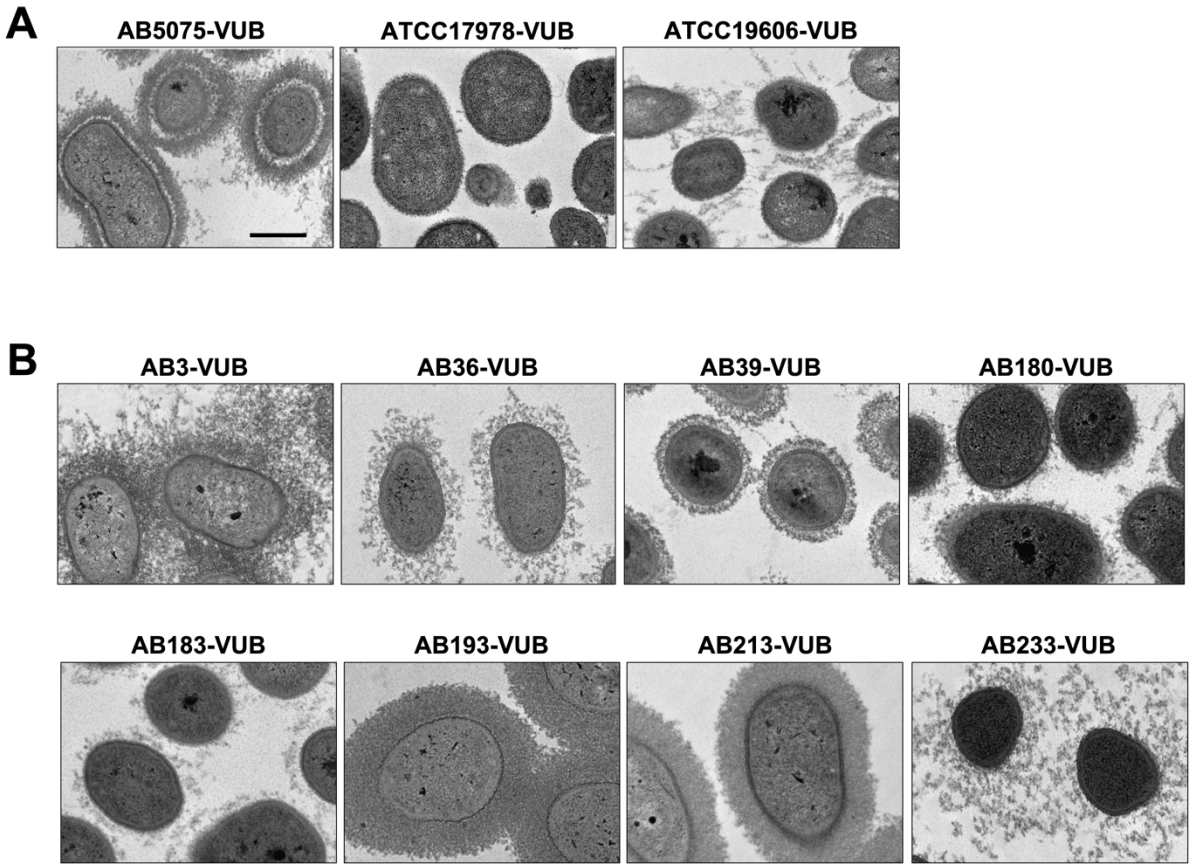

392

393 **Figure 5:** A TEM direct capsule visualization of three reference strains (A) and 8 modern clinical strains (B) of

394 various cell densities. Scale bar: 500 nm.

395

396 **Constitutive mucoid strains are not hyper-virulent**

397 As constitutive mucoid strains were observed only amongst the group of the modern MDR

398 clinical isolates, we wondered if this phenotype could be associated with a higher *in vivo*

399 virulence potential. *Galleria mellonella* larvae were infected with highly, medium, and weakly

400 capsulated isolates, while the AB5075-VUB reference strain was used as a positive control of

401 virulence (Jacobs et al., 2014). Concerning the constitutive mucoid isolates, while the AB213-

402 VUB is highly virulent, the constitutive mucoid isolates AB3-VUB and AB233-VUB are

403 weakly virulent (Figure 6). The medium capsulated isolate AB39-VUB was highly virulent and

404 killed 100% of the larvae within one day, being even more virulent than the AB5075-VUB,

405 while the medium capsulated AB36-VUB showed an intermediary virulence level.
406 Interestingly, the low capsulated isolates (AB183-VUB and AB180-VUB) were the less
407 virulent, AB180-VUB being avirulent in the tested conditions (Figure 6). These data show that
408 a constitutive high capsulation and mucoid phenotype does not correlate with a higher virulence
409 potential in *A. baumannii*. However, this highlights that low capsulation levels characterizes
410 weakly virulent phenotypes, showing that *A. baumannii* bacteria required capsule deposition
411 for full virulence. This is in agreement with previous studies showing that genetically
412 manipulated capsule deficient *A. baumannii* strains have decreased virulence levels (Talyansky
413 et al., 2021; Whiteway et al., 2021). As the virulence does not directly correlate with a specific
414 KL or OCL type, we can conclude that the KL or OCL are not solely responsible for *A.*
415 *baumannii* virulence in the tested conditions, which might require multifactorial influence.
416 Taken together, these observations show that the reference strain AB5075 is a good bacterial
417 model to study the virulence potential in *G. mellonella* while the less virulent strains
418 ATCC19606 and ATCC17978 may be used in studies tackling down the modern clinical
419 isolates exhibiting decreased virulence in *G. mellonella*.
420

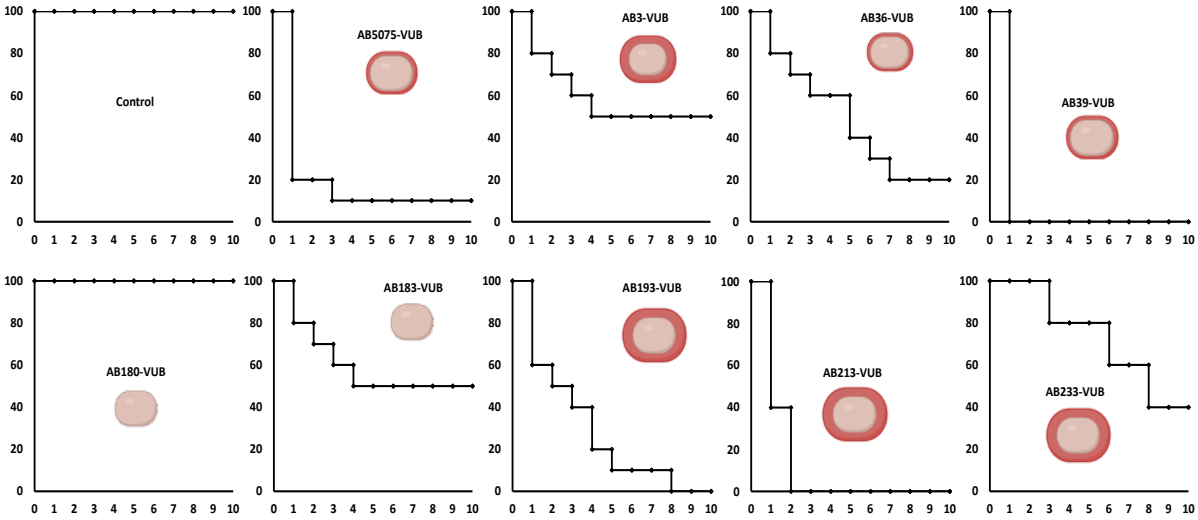

421

422 **Figure 6:** *In vivo* virulence of several modern *A. baumannii* isolates determined in *G. mellonella* model. X axis,

423 days after inoculation and Y axis, percentage of living *G. mellonella*. The control condition is the PS without
424 bacteria.
425

426 Discussion

427 The 43 modern MDR clinical isolates and four reference strains of *A. baumannii* were whole-
428 genome sequenced, *de novo* assembled and analyzed in the context of genotype and phenotype.
429 We identified 12 different ST groups in our collection of 43 modern clinical isolates. While the
430 reference strain AB5075-VUB belonged to less frequently occurring ST1 the reference strains
431 ATCC19606-VUB (ST52), ATCC17978-VUB (ST437) and DSM30011-VUB (ST738) did not
432 reflect the current trends of ST in clinical settings but rather rare sequence types. The lack of
433 representation of the ST of the clinical isolates is expectable only in the case of DSM30011-
434 VUB as this strain has environmental origin (plant microbiota). The ST2 group, previously
435 described as one important and clinically relevant group is also the most widely disseminated
436 ST among the complete and draft genomes available (Hamidian and Nigro, 2019). Most of the
437 modern clinical isolates of our collection belonged to ST2, yet none of the reference strains
438 represented this sequence type.
439 Our phylogenetic analysis (Figure 1) identified several clades, mostly in accordance with the
440 ST of the isolates. However, the reference strains DSM30011-VUB, ATCC17978-VUB and
441 ATCC19606-VUB formed a cluster with the least abundant sequence types of the clinical
442 isolates of *A. baumannii* [except AB226-VUB (ST604)]. Only this cluster consisted of the
443 isolates which all lacked *adeC* and *bauA* genes which are discussed below, suggesting an
444 extreme genetic diversity which represents only a minor proportion of the current clinical
445 isolates of *A. baumannii*. On the other hand, from the four reference strains, only AB5075-VUB
446 was the most similar to the modern clinical strains of *A. baumannii* in regard to OCL and
447 virulence genes. When considering AB5075-VUB capsule production, its phenotype was

448 resembling phenotypes of the clinical isolates with low production. Nevertheless, similarly to
449 the other reference strains, it lacked *bauA* and *adeC*. The lack of the combination of these two
450 virulence genes was also detected in ten modern clinical isolates proving that AB5075-VUB
451 still shares partial similarity with circulating clinical strains of *A. baumannii*. The described and
452 listed virulence genes in our study only account for a small amount of the virulence genes as
453 only known can be detected and possibly novel virulence genes remain to be identified.
454 Noteworthy, regardless of observed discrepancy in detection of *adeFGH* operon using VFDB
455 2022 and MEGARes 2.0 databases, the absence of *adeFGH* was described previously (Ardehali
456 et al., 2019; Coyne et al., 2010).
457 Capsule heterogeneity is a landmark of *A. baumannii* bacteria. The surface polysaccharides
458 play key roles in fitness and virulence of *A. baumannii* and protects it from the environment,
459 increases resistance to antimicrobial compounds and helps to evade the host immune system
460 (Geisinger and Isberg, 2015; Weber et al., 2016). There are more than 128 KL types identified
461 so far, and this variability demonstrates the diversity which must be surveilled in the modern
462 clinical isolates as the capsular polysaccharide is a potential target for therapeutical agents and
463 vaccines (Yang et al., 2017). In our collection of 43 modern clinical isolates of MDR *A.*
464 *baumannii*, KL40 (10/43) dominated while KL3 was detected in five isolates.
465 In our study, the most prevalent locus encoding outer-core lipooligosaccharide (OCL) type in
466 the modern clinical isolates of MDR *A. baumannii* was OCL1 (31/43). However, none of the
467 reference strains represented this most prevalent OCL1 type as they belonged to OCL2
468 (AB5075-VUB and ATCC17978-VUB), OCL3 (ATCC19606-VUB) and OCL6 (DSM30011-
469 VUB) suggesting their rarefaction in following the current epidemiological trends.
470 Two reference strains (DSM30011-VUB and AB5075-VUB) in this study lacked *bap* gene
471 encoding biofilm associated protein which could influence the studies exploring biofilm
472 properties using these reference strains. However, the gene *bap* was found in ATCC17978-

473 VUB and ATCC19606-VUB with 86% identity (VFDB 2022) same as in three clinical isolates
474 (AB40-VUB, AB32-VUB and AB21-VUB), therefore assigned as undetected in the Figure 1
475 as the identity falls under the applied threshold if 90%. The *bap* encodes protein required for
476 formation of three-dimensional biofilm towers and water channels on abiotic and biotic surfaces
477 such as polypropylene, polystyrene, and titanium (Brossard and Campagnari, 2012). Bap
478 protein is also involved in adherence of *A. baumannii* to human bronchial epithelial cells and
479 human neonatal keratinocytes (Brossard and Campagnari, 2012). Moreover, nearly half of the
480 examined strains (20/47) including four reference strain did not carry *bauA* encoding iron-
481 regulated outer membrane protein BauA. BauA protein provides protection against sepsis
482 caused by *A. baumannii* and was also identified as a vaccine candidate (Aghajani et al., 2019;
483 Ni et al., 2017). Interestingly, six strains (including two reference strains DSM30011-VUB,
484 ATCC19606-VUB and four clinical isolates AB177-VUB, AB186-VUB, AB40-VUB and
485 AB21-VUB) encoded membrane fusion protein MexE protein, part of RND efflux pump from
486 *Pseudomonas aeruginosa* (Köhler et al., 1999). Notably, the very same six strains were lacking
487 a gene encoding membrane fusion protein AdeF from AdeFGH RND efflux pump, possibly
488 restoring its function as AdeF and MexE share 50% homology. However, using the VFDB 2022
489 database, all clinical isolates and reference strains encoded *adeFGH* operon.
490 The deficiency of the clinical isolates and the reference strains in hemolytic and protease
491 activities is in agreement with the fact that only some species of *Acinetobacter* genus, e.g.,
492 *Acinetobacter haemolyticus* (Touchon et al., 2014) are capable of such phenotype. Even despite
493 this shared phenotypical trait, there was a high level of diversity of macrocolonies, where the
494 reference strains represented only two variants out of five types observed in the clinical strains.
495 Several modern isolates show a constitutive mucoid phenotype that is not observed in the
496 reference strains. Isolates belonging to the same clusters (Figure 1) do not show the same
497 ultrastructure, showing a high diversity even within the same phylogenetic group. To be noted,

498 also external events such as gene disruption can affect the phenotype of the macrocolony, as
499 was observed in AB5075-UW by Perez-Varela (Pérez-Varela et al., 2020) by disrupting *relA*
500 ortholog (*ABUW_3302*) using transposon insertion. Taken together, this points out the
501 insufficiency of the reference strains in grasping the complete phenotypical (and genotypical)
502 diversity of the modern clinical isolates.
503 The natural competence for transformation is one of the ways of horizontal gene transfer *A.*
504 *baumannii* uses to acquire extracellular DNA from the environment and incorporates it into its
505 own genome via homologous recombination (Dubnau and Blokesch, 2019). We observed that
506 the competence to be naturally transformed varied within clinical isolates of *A. baumannii* from
507 which 13 were transformed, 18 were not and 12 were intrinsically resistant to apramycin,
508 therefore unable to assess. This diverse trend was copied by the reference strains as well as
509 AB5075-VUB and DSM30011-VUB were successfully transformed while ATCC17978-VUB
510 was not and ATCC19696-VUB showed intrinsic resistance to apramycin. There are multiple
511 factors influencing the ability of *A. baumannii* to be naturally transformed such as presence of
512 the H-NS (Le et al., 2021) which was present in each case within our isolates and strains.
513 However, the major role is played by type IV pilus genes (Leong et al., 2017) which are growth
514 phase dependent (Vesel and Blokesch, 2021), and might be the explanation of some isolates
515 and strains not being transformed. However, the tested conditions of natural competence were
516 standardized pointing out further physiological diversity within *A. baumannii* clinical isolates
517 and reference strains. Despite the proven relevance of the clinical isolates of our collection
518 (collected as problematic and modern nosocomial isolates), we cannot rule out a bias to certain
519 extend.
520 We observe a high diversity in production of the capsular polysaccharide using direct and
521 indirect visualization methods. We show a correlation between capsule abundance and density
522 levels, but correlation does not mean causation. We cannot rule out the possibility that the

523 capsule type *per se* (and not only the capsule abundance) or other factors, influence the density
524 of *A. baumannii* bacteria. The fact that widely used reference strains show low to medium
525 encapsulation degrees add an additional reason why reference strains should be carefully used
526 and argue in favor of considering the strain AB5075-VUB as the best representative bacterial
527 model out of the four reference strains tested in this study. However, a rather complex solution
528 to selection of proper strain to be used in a specific study is needed such as Acinetobase (Valcek
529 et al., unpublished). Acinetobase is a comprehensive database providing the community with
530 genotype, phenotype and the strain of *A. baumannii* itself.
531 The *Galleria mellonella* infection model proved itself as a valuable source of information on
532 the virulence level of *A. baumannii*. This model also highlighted AB5075-VUB to be more
533 virulent than ATCC19606-VUB and ATCC17978-VUB in the tested conditions (Jacobs et al.,
534 2014). These results support the usage of modern clinical isolates for study of virulence, hence
535 other highly virulent isolates such as hypervirulent *A. baumannii* LAC-4 (Ou et al., 2015)
536 should be considered as well.
537 As constitutive mucoid strains were observed only amongst the group of the modern MDR
538 clinical isolates, we wondered if this phenotype could be associated with a higher *in vivo*
539 virulence potential. The virulence in *G. mellonella* model varied for the tested clinical isolates
540 and the reference strains and while a constitutive mucoid phenotype does not correlate with a
541 higher virulence, we confirm using modern clinical isolates that low capsule production
542 impedes full virulence in *A. baumannii*. These observations do not confirm the results of Shan
543 et al., (Shan et al., 2021) who concluded that the mucoid *A. baumannii* isolates were more
544 hypervirulent than the nonmucoid strains. This discrepancy may point towards multifactorial
545 background of hypervirulence.

546 The signal(s) or conditions regulating capsule production remain to be determined. Noteworthy,
547 the isolates AB193-VUB and AB213-VUB with higher integrity of the CPS layer (Figure 5)
548 have shown higher virulence in *G. mellonella* (Figure 6) than isolates with dispersed CPS.
549 The study of genetic features which are not shared by the majority of *A. baumannii* isolates
550 (soft-core, shell and cloud genes (Cummins et al., 2022)) may lead to novel discoveries as well.
551 However, the global impact of the clinical importance (drug therapies or target-driven drug
552 discoveries) will suffer from linking the specific genes and features only to certain isolate or
553 lineage.
554

555 # Conclusion

556 *A. baumannii* are heterogenous bacteria, both at the genetic and phenotypic levels. In this study,
557 we characterized 43 modern clinical isolates from different phylogenetic groups and 4 reference
558 strains with common but also very different behaviors. Therefore, the reference strains tested
559 in our study do not cover the whole heterogeneity found in the modern isolates of *A. baumannii*.
560 The studies previously published using these reference strains built a strong state of the art in
561 the *A. baumannii* field and beyond, showing their usefulness. However, the data presented in
562 our study show that the specific use of one or only a limited subset of reference strains can
563 hinder important processes characterizing clinically relevant isolates and the *A. baumannii*
564 bacteria as a whole. As an answer to that identified pitfall, we propose a variable collection of
565 modern clinical isolates that are characterized at the genetic and phenotypic levels, covering
566 the full range of the phenotypic spectrum, with five different macrocolony type groups, from
567 avirulent to hyper virulent phenotype, and with non-capsulated to hyper mucoid strains, with
568 intermediate phenotypes as well. This will allow selecting a reference strain rationally,
569 facilitated by the new Acinetobase (Valcek et al., unpublished) platform, which suits the needs
570 of an ongoing study with a particular biological question. This is especially important for new

571 antimicrobial screening purposes, for which conserved targets amongst a significant proportion
572 of problematic *A. baumannii* isolates is a prerequisite. While strain specific observation remains
573 interesting *per se*, in the context of such a drastic heterogeneity, any new identified target,
574 antimicrobial compound, or fundamental observation deserved to be tested on diverse relevant
575 *A. baumannii* isolates.
576
577
578
579
580

581 # Data availability

582 The short- and long-read sequences were deposited in GenBank under BioProject
583 PRJNA734485 and PRJNA798866, respectively.
584

585 # Funding

586 This project was supported by the Flanders Institute for Biotechnology (VIB) and has received
587 funding from the European Union's Horizon 2020 research and innovation program under the
588 Marie Sklodowska-Curie grant agreement No 748032. KN was supported by the Erasmus +
589 program KA131-HED.
590

591 # Acknowledgements

592 We are grateful to the URBM and URBE research groups, as well as the Electron Microscopy
593 Service from UNamur, for the access to their equipment and their expertise. We thank Ivan
594 Mateus from the Department of Ecology and Evolution, University of Lausanne, Lausanne,

Switzerland for a fruitful discussion of initial bioinformatical analyses. We thank the National Reference Laboratory for Monitoring of Antimicrobial Resistance in Gram-negative Bacteria, CHU Mont-Godinne, Université Catholique de Louvain (UCL), Yvoir (Belgium) for providing the modern clinical isolates.

Competing interests

None to declare.

Contribution

CP, CVDH and ER performed phenotypical experiments. AV, CVDH and KN performed bioinformatical analyses. CW extracted DNA for the long-read sequencing. MB, CP, CVDH and TC performed the infections of *Galleria mellonella*. TDP, WDC and MS set up the LRS strategy, sample, library preparation and sequencing. JK provided her expertise in KL and OCL identification. AV and CVDH wrote the manuscript

References

Aghajani Z, Rasooli I, Mousavi Gargari SL. 2019. Exploitation of two siderophore receptors, BauA and BfnH, for protection against *Acinetobacter baumannii* infection. *APMIS* **127**:753–763. doi:10.1111/apm.12992

Arbatsky NP, Shneider MM, Kenyon JJ, Shashkov AS, Popova A v., Miroshnikov KA, Volozhantsev N v., Knirel YA. 2015. Structure of the neutral capsular polysaccharide of *Acinetobacter baumannii* NIPH146 that carries the KL37 capsule gene cluster. *Carbohydrate Research* **413**:12–15. doi:10.1016/J.CARRES.2015.05.003

Ardehali SH, Azimi T, Fallah F, Owrang M, Aghamohammadi N, Azimi L. 2019. Role of efflux pumps in reduced susceptibility to tigecycline in *Acinetobacter baumannii*. *New Microbes and New Infections* **30**:100547. doi:10.1016/J.NMNI.2019.100547

Ardissone S, Fumeaux C, Bergé M, Beaussart A, Théraulaz L, Radhakrishnan SK, Dufrêne YF, Viollier PH. 2014. Cell cycle constraints on capsulation and bacteriophage susceptibility. *eLife* **3**:1–30. doi:10.7554/ELIFE.03587

625 Bolger AM, Lohse M, Usadel B. 2014. Trimmomatic: A flexible trimmer for Illumina sequence
626 data. *Bioinformatics* **30**:2114–2120. doi:10.1093/bioinformatics/btu170
627 Boll JM, Tucker AT, Klein DR, Beltran AM, Brodbelt JS, Davies BW, Trent MS. 2015.
628 Reinforcing lipid a acylation on the cell surface of *Acinetobacter baumannii* promotes
629 cationic antimicrobial peptide resistance and desiccation survival. *mBio* **6**:1–11.
630 doi:10.1128/MBIO.00478-15/SUPPL_FILE/MBO003152328ST2.PDF
631 Bortolaia V, Kaas RS, Ruppe E, Roberts MC, Schwarz S, Cattoir V, Philippon A, Allesoe RL,
632 Rebelo AR, Florensa AF, Fagelhauer L, Chakraborty T, Neumann B, Werner G, Bender
633 JK, Stingl K, Nguyen M, Coppens J, Xavier BB, Malhotra-Kumar S, Westh H, Pinholt M,
634 Anjum MF, Duggett NA, Kempf I, Nykäsenoja S, Olkkola S, Wieczorek K, Amaro A,
635 Clemente L, Mossong J, Losch S, Ragimbeau C, Lund O, Aarestrup FM. 2020. ResFinder
636 4.0 for predictions of phenotypes from genotypes. *Journal of Antimicrobial Chemotherapy*
637 **75**:3491–3500. doi:10.1093/JAC/DKAA345
638 Bouvet PJM, Grimont PAD. 1986. Taxonomy of the Genus *Acinetobacter* with the Recognition
639 of *Acinetobacter baumannii* sp. nov., Acinetobacter haemolyticus sp. nov., Acinetobacter
640 johnsonii sp. nov., and *Acinetobacter junii* sp. nov. and Emended Descriptions of
641 *Acinetobacter calcoaceticus* and *Acinetobacter lwoffii*. *International Journal of*
642 *Systematic and Evolutionary Microbiology* **36**:228–240. doi:10.1099/00207713-36-2-228
643 Bravo Z, Orruño M, Parada C, Kaberdin VR, Barcina I, Arana I. 2016. The long-term survival
644 of *Acinetobacter baumannii* ATCC 19606T under nutrient-deprived conditions does not
645 require the entry into the viable but non-culturable state. *Archives of Microbiology*
646 **198**:399–407. doi:10.1007/s00203-016-1200-1
647 Brossard KA, Campagnari AA. 2012. The *Acinetobacter baumannii* Biofilm-Associated
648 Protein Plays a Role in Adherence to Human Epithelial Cells. doi:10.1128/IAI.05913-11
649 Centers for Disease Control U. 2019. Antibiotic Resistance Threats in the United States, 2019.
650 doi:10.15620/cdc:82532
651 Chiang SR, Jung F, Tang HJ, Chen CH, Chen CC, Chou HY, Chuang YC. 2018. Desiccation
652 and ethanol resistances of multidrug resistant *Acinetobacter baumannii* embedded in
653 biofilm: The favorable antiseptic efficacy of combination chlorhexidine gluconate and
654 ethanol. *Journal of Microbiology, Immunology and Infection* **51**:770–777.
655 doi:10.1016/j.jmii.2017.02.003
656 Chin CY, Tipton KA, Farokhyfar M, Burd EM, Weiss DS, Rather PN. 2018. A high-frequency
657 phenotypic switch links bacterial virulence and environmental survival in *Acinetobacter*
658 *baumannii*. *Nature Microbiology 2018 3:5* **3**:563–569. doi:10.1038/s41564-018-0151-5
659 Coyne S, Rosenfeld N, Lambert T, Courvalin P, Périchon B. 2010. Overexpression of
660 resistance-nodulation-cell division pump AdeFGH confers multidrug resistance in
661 *Acinetobacter baumannii*. *Antimicrobial Agents and Chemotherapy* **54**:4389–4393.
662 doi:10.1128/AAC.00155-10/ASSET/051BDFEF-DB1A-4F55-B6EB-
663 323DD38348B4/ASSETS/GRAPHIC/ZAC9991093410002.JPEG
664 Cummins EA, Hall RJ, McInerney JO, McNally A. 2022. Prokaryote pangenomes are dynamic
665 entities. *Current Opinion in Microbiology* **66**:73–78. doi:10.1016/J.MIB.2022.01.005
666 da Silva G, Domingues S. 2016. Insights on the Horizontal Gene Transfer of Carbapenemase
667 Determinants in the Opportunistic Pathogen *Acinetobacter baumannii*. *Microorganisms*
668 **4**:29. doi:10.3390/microorganisms4030029
669 de Coster W, D'hert S, Schultz DT, Cruts M, van Broeckhoven C. 2018. NanoPack: visualizing
670 and processing long-read sequencing data. doi:10.1093/bioinformatics/bty149
671 de Oliveira DMP, Forde BM, Kidd TJ, Harris PNA, Schembri MA, Beatson SA, Paterson DL,
672 Walker MJ. 2020. Antimicrobial Resistance in ESKAPE Pathogens. doi:10.1128/CMR

673 de Silva PM, Chong P, Fernando DM, Westmacott G, Kumar A. 2017. Effect of Incubation
674 Temperature on Antibiotic Resistance and Virulence Factors of *Acinetobacter baumannii*
675 ATCC 17978. doi:10.1128/AAC.01514-17
676 Dong C, Beis K, Nesper J, Brunkan AL, Clarke BR, Whitfield C, Naismith JH. 2006. The
677 structure of Wza, the translocon for group 1 capsular polysaccharides in *Escherichia coli*,
678 identifies a new class of outer membrane protein. *Nature* **444**:226.
679 doi:10.1038/NATURE05267
680 Doster E, Lakin SM, Dean CJ, Wolfe C, Young JG, Boucher C, Belk KE, Noyes NR, Morley
681 PS. 2020. MEGARes 2.0: A database for classification of antimicrobial drug, biocide and
682 metal resistance determinants in metagenomic sequence data. *Nucleic Acids Research*
683 **48**:D561–D569. doi:10.1093/nar/gkz1010
684 Dubnau D, Blokesch M. 2019. Mechanisms of DNA Uptake by Naturally Competent Bacteria.
685 *https://doi.org/101146/annurev-genet-112618-043641* **53**:217–237.
686 doi:10.1146/ANNUREV-GENET-112618-043641
687 Gaiarsa S, Batisti Biffignandi G, Esposito EP, Castelli M, Jolley KA, Brisse S, Sassera D,
688 Zarrilli R. 2019. Comparative analysis of the two *Acinetobacter baumannii* multilocus
689 sequence typing (MLST) schemes. *Frontiers in Microbiology* **10**.
690 doi:10.3389/fmicb.2019.00930
691 Gallagher LA, Ramage E, Weiss EJ, Radey M, Hayden HS, Held KG, Huse HK, Zurawski D
692 v., Brittnacher MJ, Manoil C. 2015. Resources for genetic and genomic analysis of
693 emerging pathogen *Acinetobacter baumannii*. *Journal of Bacteriology* **197**:2027–2035.
694 doi:10.1128/JB.00131-15
695 Geisinger E, Huo W, Hernandez-Bird J, Isberg RR. 2019. *Acinetobacter baumannii*: Envelope
696 Determinants That Control Drug Resistance, Virulence, and Surface Variability.
697 *https://doi.org/101146/annurev-micro-020518-115714* **73**:481–506.
698 doi:10.1146/ANNUREV-MICRO-020518-115714
699 Geisinger E, Isberg RR. 2015. Antibiotic Modulation of Capsular Exopolysaccharide and
700 Virulence in *Acinetobacter baumannii*. *PLOS Pathogens* **11**:e1004691.
701 doi:10.1371/journal.ppat.1004691
702 Hamidian M, Nigro SJ. 2019. Emergence, molecular mechanisms and global spread of
703 carbapenem-resistant *Acinetobacter baumannii*. *Microbial Genomics*.
704 doi:10.1099/mgen.0.000306
705 Harding CM, Hennon SW, Feldman MF. 2017. Uncovering the mechanisms of *Acinetobacter*
706 *baumannii* virulence. *Nature Reviews Microbiology 2017 16:2* **16**:91–102.
707 doi:10.1038/nrmicro.2017.148
708 Hernando-Amado S, Coque TM, Baquero F, Martínez JL. 2019. Defining and combating
709 antibiotic resistance from One Health and Global Health perspectives. *Nature*
710 *Microbiology*. doi:10.1038/s41564-019-0503-9
711 Holley G, Beyter D, Ingimundardottir H, Møller PL, Kristmundsdottir S, Eggertsson HP,
712 Halldorsson B v. 2021. Ratatosk: hybrid error correction of long reads enables accurate
713 variant calling and assembly. *Genome Biology* **22**:1–22. doi:10.1186/S13059-020-02244-
714 4/FIGURES/8
715 Imperi F, Antunes LCS, Blom J, Villa L, Iacono M, Visca P, Carattoli A. 2011. The genomics
716 of *Acinetobacter baumannii*: Insights into genome plasticity, antimicrobial resistance and
717 pathogenicity. *IUBMB Life* **63**:1068–1074. doi:10.1002/iub.531
718 Jacobs AC, Thompson MG, Black CC, Kessler JL, Clark LP, McQueary CN, Gancz HY, Corey
719 BW, Moon JK, Si Y, Owen MT, Hallock JD, Kwak YI, Summers A, Li CZ, Rasko DA,
720 Penwell WF, Honnold CL, Wise MC, Waterman PE, Lesho EP, Stewart RL, Actis LA,
721 Palys TJ, Craft DW, Zurawski D v. 2014. AB5075, a highly virulent isolate of

722 *Acinetobacter baumannii*, as a model strain for the evaluation of pathogenesis and
723 antimicrobial treatments. *mBio* **5**. doi:10.1128/mBio.01076-14
724 Kenyon JJ, Hall RM. 2013. Variation in the Complex Carbohydrate Biosynthesis Loci of
725 *Acinetobacter baumannii* Genomes. *PLoS ONE* **8**:e62160.
726 doi:10.1371/journal.pone.0062160
727 Kenyon JJ, Nigro SJ, Hall RM. 2014. Variation in the OC Locus of *Acinetobacter baumannii*
728 Genomes Predicts Extensive Structural Diversity in the Lipooligosaccharide. *PLoS ONE*
729 **9**:e107833. doi:10.1371/journal.pone.0107833
730 Köhler T, Epp SF, Curty LK, Pechère JC. 1999. Characterization of MexT, the regulator of the
731 MexE-MexF-OprN multidrug efflux system of *Pseudomonas aeruginosa*. *Journal of*
732 *Bacteriology* **181**:6300–6305. doi:10.1128/jb.181.20.6300-6305.1999
733 Kolmogorov M, Yuan J, Lin Y, Pevzner PA. 2019. Assembly of long, error-prone reads using
734 repeat graphs. *Nature Biotechnology* **37**:540–546. doi:10.1038/s41587-019-0072-8
735 Kon H, Schwartz D, Temkin E, Carmeli Y, Lellouche J. 2020. Rapid identification of
736 capsulated *Acinetobacter baumannii* using a density-dependent gradient test. *BMC*
737 *Microbiology* **20**:1–11. doi:10.1186/s12866-020-01971-9
738 Le C, Pimentel C, Tuttobene MR, Subils T, Escalante J, Nishimura B, Arriaga S, Rodgers D,
739 Bonomo RA, Sieira R, Tolmasky ME, Ramírez MS. 2021. Involvement of the Histone-
740 Like Nucleoid Structuring Protein (H-NS) in *Acinetobacter baumannii*'s Natural
741 Transformation. *Pathogens 2021, Vol 10, Page 1083* **10**:1083.
742 doi:10.3390/PATHOGENS10091083
743 Leong CG, Bloomfield RA, Boyd CA, Dornbusch AJ, Lieber L, Liu F, Owen A, Slay E, Lang
744 KM, Lostroh CP. 2017. The role of core and accessory type IV pilus genes in natural
745 transformation and twitching motility in the bacterium *Acinetobacter baylyi*. *PLOS ONE*
746 **12**:e0182139. doi:10.1371/JOURNAL.PONE.0182139
747 Letunic I, Bork P. 2019. Interactive Tree of Life (iTOL) v4: Recent updates and new
748 developments. *Nucleic Acids Research* **47**:W256–W259. doi:10.1093/nar/gkz239
749 Liu B, Zheng D, Zhou S, Chen L, Yang J. 2022. VFDB 2022: a general classification scheme
750 for bacterial virulence factors. *Nucleic Acids Research* **50**:D912–D917.
751 doi:10.1093/NAR/GKAB1107
752 Murray CJ, Ikuta KS, Sharara F, Swetschinski L, Robles Aguilar G, Gray A, Han C, Bisignano
753 C, Rao P, Wool E, Johnson SC, Browne AJ, Chipeta MG, Fell F, Hackett S, Haines-
754 Woodhouse G, Kashef Hamadani BH, Kumaran EAP, McManigal B, Agarwal R, Akech
755 S, Albertson S, Amuasi J, Andrews J, Aravkin A, Ashley E, Bailey F, Baker S, Basnyat
756 B, Bekker A, Bender R, Bethou A, Bielicki J, Boonkasidecha S, Bukosia J, Carvalheiro
757 C, Castañeda-Orjuela C, Chansamouth V, Chaurasia S, Chiurchiù S, Chowdhury F, Cook
758 AJ, Cooper B, Cressey TR, Criollo-Mora E, Cunningham M, Darboe S, Day NPJ, de Luca
759 M, Dokova K, Dramowski A, Dunachie SJ, Eckmanns T, Eibach D, Emami A, Feasey N,
760 Fisher-Pearson N, Forrest K, Garrett D, Gastmeier P, Giref AZ, Greer RC, Gupta V, Haller
761 S, Haselbeck A, Hay SI, Holm M, Hopkins S, Iregbu KC, Jacobs J, Jarovsky D,
762 Javanmardi F, Khorana M, Kissoon N, Kobeissi E, Kostyanev T, Krapp F, Krumkamp R,
763 Kumar A, Kyu HH, Lim C, Limmathurotsakul D, Loftus MJ, Lunn M, Ma J, Mturi N,
764 Munera-Huertas T, Musicha P, Mussi-Pinhata MM, Nakamura T, Nanavati R, Nangia S,
765 Newton P, Ngoun C, Novotney A, Nwakanma D, Obiero CW, Olivas-Martinez A, Olliaro
766 P, Ooko E, Ortiz-Brizuela E, Peleg AY, Perrone C, Plakkal N, Ponce-de-Leon A, Raad M,
767 Ramdin T, Riddell A, Roberts T, Robotham JV, Roca A, Rudd KE, Russell N, Schnall J,
768 Scott JAG, Shivamallappa M, Sifuentes-Osornio J, Steenkeste N, Stewardson AJ, Stoeva
769 T, Tasak N, Thaiprakong A, Thwaites G, Turner C, Turner P, van Doorn HR, Velaphi S,
770 Vongpradith A, Vu H, Walsh T, Waner S, Wangrangsimakul T, Wozniak T, Zheng P,
771 Sartorius B, Lopez AD, Stergachis A, Moore C, Dolecek C, Naghavi M. 2022. Global

burden of bacterial antimicrobial resistance in 2019: a systematic analysis. *The Lancet* **399**:629–655. doi:10.1016/S0140-6736(21)02724-0

Ni Z, Chen Y, Ong E, He Y. 2017. Antibiotic resistance determinant-focused *Acinetobacter baumannii* vaccine designed using reverse vaccinology. *International Journal of Molecular Sciences* **18**. doi:10.3390/ijms18020458

Niu T, Guo L, Luo Q, Zhou K, Yu W, Chen Y, Huang C, Xiao Y. 2019. Wza gene knockout decreases *Acinetobacter baumannii* virulence and affects Wzy-dependent capsular polysaccharide synthesis. *https://doi.org/101080/2150559420191700659* **11**:1–13. doi:10.1080/21505594.2019.1700659

Ou HY, Kuang SN, He X, Molgora BM, Ewing PJ, Deng Z, Osby M, Chen W, Xu HH. 2015. Complete genome sequence of hypervirulent and outbreak-associated *Acinetobacter baumannii* strain LAC-4: epidemiology, resistance genetic determinants and potential virulence factors. *Scientific Reports 2015 5:1* **5**:1–13. doi:10.1038/srep08643

Page AJ, Cummins CA, Hunt M, Wong VK, Reuter S, Holden MTG, Fookes M, Falush D, Keane JA, Parkhill J. 2015. Roary: Rapid large-scale prokaryote pan genome analysis. *Bioinformatics* **31**:3691–3693. doi:10.1093/bioinformatics/btv421

Pérez-Varela M, Tierney ARP, Kim J-S, Vázquez-Torres A, Rather P. 2020. Characterization of RelA in *Acinetobacter baumannii*. doi:10.1128/JB.00045-20

Poirel L, Nordmann P. 2006. Carbapenem resistance in *Acinetobacter baumannii*: Mechanisms and epidemiology. *Clinical Microbiology and Infection*. doi:10.1111/j.1469-0691.2006.01456.x

Repizo GD, Viale AM, Borges V, Cameranesi MM, Taib N, Espariz M, Brochier-Armanet C, Gomes JP, Salcedo SP. 2017. The Environmental *Acinetobacter baumannii* Isolate DSM30011 Reveals Clues into the Preantibiotic Era Genome Diversity, Virulence Potential, and Niche Range of a Predominant Nosocomial Pathogen. *Genome Biology and Evolution* **9**:2292–2307. doi:10.1093/GBE/EVX162

Roussin M, Rabarioelina S, Cluzeau L, Cayron J, Lesterlin C, Salcedo SP, Bigot S. 2019. Identification of a Contact-Dependent Growth Inhibition (CDI) System That Reduces Biofilm Formation and Host Cell Adhesion of *Acinetobacter baumannii* DSM30011 Strain. *Frontiers in Microbiology* **10**:2450. doi:10.3389/fmicb.2019.02450

Sarshar M, Behzadi P, Scribano D, Palamara AT, Ambrosi C. 2021. *Acinetobacter baumannii*: An Ancient Commensal with Weapons of a Pathogen. *Pathogens 2021, Vol 10, Page 387* **10**:387. doi:10.3390/PATHOGENS10040387

Seemann T. 2014. Prokka: Rapid prokaryotic genome annotation. *Bioinformatics* **30**:2068–2069. doi:10.1093/bioinformatics/btu153

Senchenkova SN, Shashkov AS, Popova A v., Shneider MM, Arbatsky NP, Miroshnikov KA, Volozhantsev N v., Knirel YA. 2015. Structure elucidation of the capsular polysaccharide of *Acinetobacter baumannii* AB5075 having the KL25 capsule biosynthesis locus. *Carbohydrate Research* **408**:8–11. doi:10.1016/J.CARRES.2015.02.011

Shan W, Zhang H, Kan J, Yin M, Zhang J, Wan L, Chang R, Li M. 2021. Acquired mucoid phenotype of *Acinetobacter baumannii*: Impact for the molecular characteristics and virulence. *Microbiological Research* **246**:126702. doi:10.1016/J.MICRES.2021.126702

Stamatakis A. 2006. RAxML-VI-HPC: Maximum likelihood-based phylogenetic analyses with thousands of taxa and mixed models. *Bioinformatics* **22**:2688–2690. doi:10.1093/bioinformatics/btl446

Tacconelli E, Carrara E, Savoldi A, Harbarth S, Mendelson M, Monnet DL, Pulcini C, Kahlmeter G, Kluytmans J, Carmeli Y, Ouellette M, Outterson K, Patel J, Cavaleri M, Cox EM, Houchens CR, Grayson L, Hansen P, Singh N, Theuretzbacher U, Magrini N. 2018. Discovery, research, and development of new antibiotics: the WHO priority list of

821 antibiotic-resistant bacteria and tuberculosis. *www.thelancet.com/infection* **18**.
822 doi:10.1016/S1473-3099(17)30753-3
823 Talyansky Y, Nielsen TB, Yan J, Carlino-Macdonald U, di Venanzio G, Chakravorty S, Ulhaq
824 A, Feldman MF, Russo TA, Vinogradov E, Luna B, Wright MS, Adams MD, Spellberg
825 B. 2021. Capsule carbohydrate structure determines virulence in *Acinetobacter*
826 *baumannii*. *PLOS Pathogens* **17**:e1009291. doi:10.1371/JOURNAL.PPAT.1009291
827 Tipton KA, Dimitrova D, Rather PN. 2015. Phase-variable control of multiple phenotypes in
828 *Acinetobacter baumannii* strain AB5075. *Journal of Bacteriology* **197**:2593–2599.
829 doi:10.1128/JB.00188-15
830 Touchon M, Cury J, Yoon EJ, Krizova L, Cerqueira GC, Murphy C, Feldgarden M, Wortman
831 J, Clermont D, Lambert T, Grillot-Courvalin C, Nemec A, Courvalin P, Rocha EPC. 2014.
832 The genomic diversification of the whole *Acinetobacter* genus: Origins, mechanisms, and
833 consequences. *Genome Biology and Evolution* **6**:2866–2882. doi:10.1093/gbe/evu225
834 Valcek A, Bogaerts P, Denis O, Huang T-D, Henst C van der. 2021. Molecular epidemiology
835 of carbapenem-resistant *Acinetobacter baumannii* strains in Belgian acute-care hospitals.
836 *medRxiv* 2021.07.06.21259728. doi:10.1101/2021.07.06.21259728
837 van der Henst C, Vanhove AS, Drebes Dörr NC, Stutzmann S, Stoudmann C, Clerc S, Scrignari
838 T, Maclachlan C, Knott G, Blokesch M. 2018. Molecular insights into *Vibrio cholerae*'s
839 intra-amoebal host-pathogen interactions. *Nature Communications 2018 9:1* **9**:1–13.
840 doi:10.1038/s41467-018-05976-x
841 Vesel N, Blokesch M. 2021. Pilus Production in *Acinetobacter baumannii* Is Growth Phase
842 Dependent and Essential for Natural Transformation. doi:10.1128/JB.00034-21
843 Walker BJ, Abeel T, Shea T, Priest M, Abouelliel A, Sakthikumar S, Cuomo CA, Zeng Q,
844 Wortman J, Young SK, Earl AM. 2014. Pilon: An Integrated Tool for Comprehensive
845 Microbial Variant Detection and Genome Assembly Improvement. *PLoS ONE* **9**:e112963.
846 doi:10.1371/journal.pone.0112963
847 Wang-Lin SX, Olson R, Beanan JM, MacDonald U, Balthasar JP, Russo TA. 2017. The
848 Capsular Polysaccharide of *Acinetobacter baumannii* Is an Obstacle for Therapeutic
849 Passive Immunization Strategies. *Infection and Immunity* **85**. doi:10.1128/IAI.00591-17
850 Weber BS, Harding CM, Feldman MF. 2016. Pathogenic *Acinetobacter*: from the Cell Surface
851 to Infinity and Beyond. doi:10.1128/JB.00906-15
852 Whiteway C, Breine A, Philippe C, van der Henst C. 2022. *Acinetobacter baumannii*. *Trends*
853 *in Microbiology* **30**:199–200. doi:10.1016/J.TIM.2021.11.008
854 Whiteway C, Valcek A, Philippe C, Strazisar M, de Pooter T, Mateus I, Breine A, Van der
855 Henst C. 2021. Scarless excision of an insertion sequence restores capsule production and
856 virulence in *Acinetobacter baumannii*. *The ISME Journal 2022* 1–5. doi:10.1038/s41396-
857 021-01179-3
858 Wick RR, Heinz E, Holt KE, Wyres KL, Diekema DJ. 2018. Kaptive Web: User-Friendly
859 Capsule and Lipopolysaccharide Serotype Prediction for *Klebsiella* Genomes.
860 *jcm.asm.org 1 Journal of Clinical Microbiology* **56**:197–215. doi:10.1128/JCM.00197-18
861 Wyres KL, Cahill SM, Holt KE, Hall RM, Kenyon JJ. 2020. Identification of *Acinetobacter*
862 *baumannii* loci for capsular polysaccharide (KL) and lipooligosaccharide outer core
863 (OCL) synthesis in genome assemblies using curated reference databases compatible with
864 kaptive. *Microbial Genomics* **6**:e000339. doi:10.1099/mgen.0.000339
865 Yang FL, Lou TC, Kuo SC, Wu WL, Chern J, Lee YT, Chen ST, Zou W, Lin NT, Wu SH.
866 2017. A medically relevant capsular polysaccharide in *Acinetobacter baumannii* is a
867 potential vaccine candidate. *Vaccine* **35**:1440–1447. doi:10.1016/j.vaccine.2017.01.060

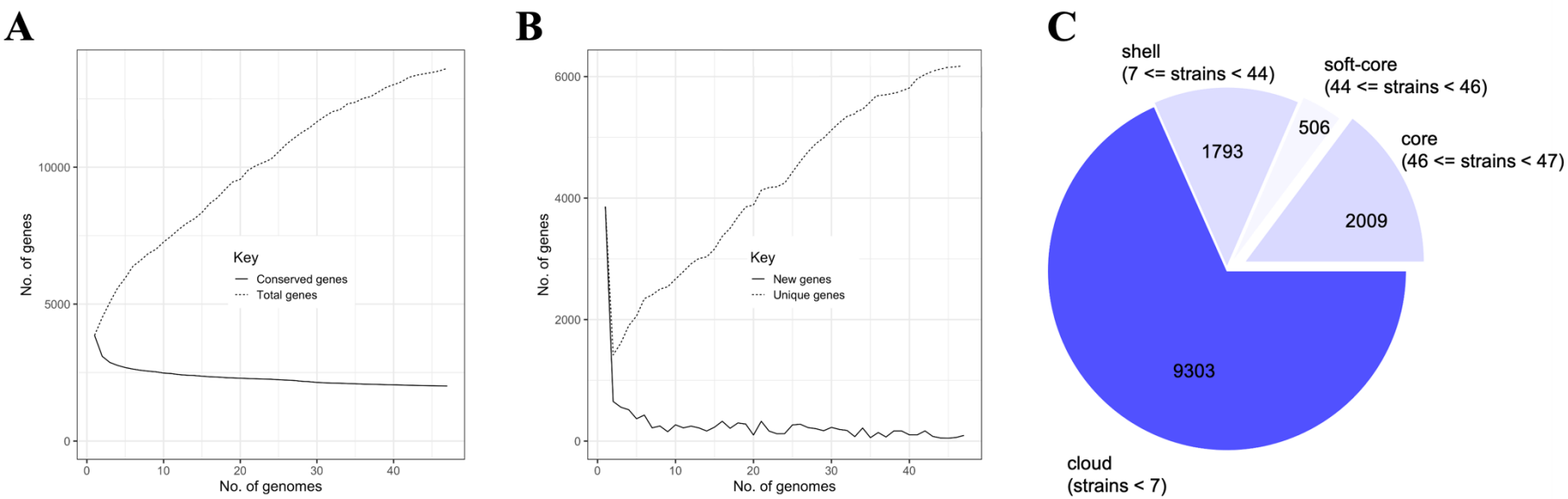

Figure 1: A depiction of (A) Conserved and total gene numbers in the pangenome. (B) Novel and unique gene numbers in the pangenome. These graphs indicate how the pangenome varies as genomes are added. (C) Pangenome pie chart showing the number of core and accessory genes. Accessory genes were divided into soft core, shell and cloud genes.

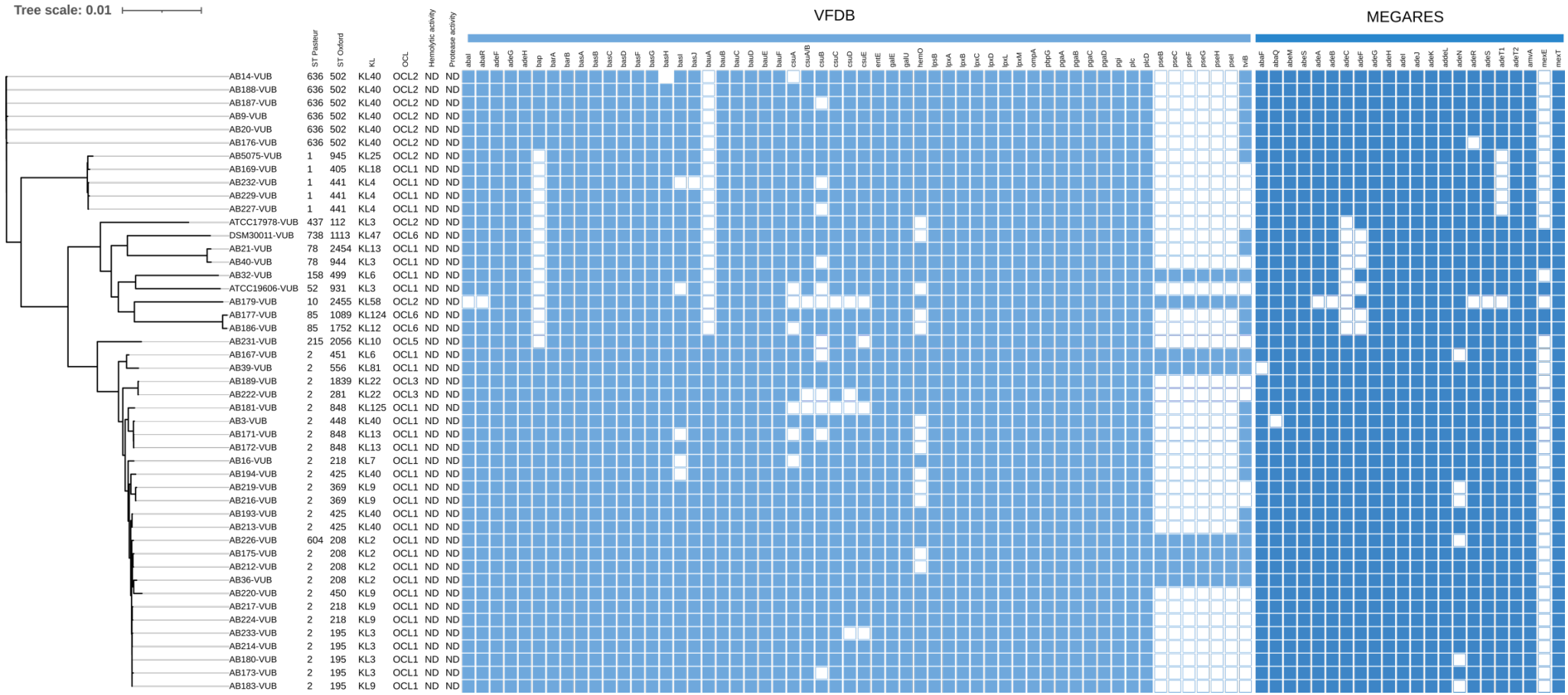

Figure 2: A phylogenetic tree of 43 modern clinical isolates and four reference strains of *A. baumannii* with depiction of ST^{Pas} and ST^{Ox}, KL, OCL, hemolytic activity, protease activity and virulence genes as detected using VFDB 2022 and MEGARes 2.0 databases, respectively. ND – Not Detected

Supplementary Figure 1: A phylogenetic tree of 43 modern clinical isolates and four reference strains of *A. baumannii* with depiction of ST^{Pas} and ST^{Ox}, KL, OCL, hemolytic activity, protease activity and resistance genes, respectively. ND – Not Detected